

Spatial Distribution Mapping by Mobile Sensor Networks: A Bayesian Method

Hyongju Park, Matthew Johnson-Roberson and Ram Vasudevan

Abstract—(**Ram:** need just one sentence that describes what environmental mapping is and why its important.) Though such environmental mapping tasks can be done efficiently via dispatching a group of autonomous agents, it is typically undertaken by humans due to the lack of formal methods that are able to guarantee (**Ram:** need details here about what is the missing piece for existing methods). This paper presents a Bayesian approach to estimating spatially distributed target maps by deploying a group of mobile robots, as motivated by the example. The topological (locations) and spatial properties (e.g., radiation level, magnetic field strength, temperature levels, etc) which constitute the target state are unknown and are characterized by prior probability distribution over bounded domain. This paper proposes a deterministic motion model wherein robots move to maximize the observation likelihood based on their noisy sensor measurements and prior beliefs on target state. In addition, a decentralized counterpart, suitable for short range sensors, is presented wherein the workspace is partitioned into multiple disjoint regions, and each robot detects target only in its associated region. Both simulation results and real-world validation are presented to demonstrate the effectiveness of the proposed methods.

I. INTRODUCTION

A team of mobile robots equipped with ad-hoc communication and sensing devices, a *Mobile Sensor Network* (MSN), has a wide range of potential applications, including, exploration, surveillance, search and rescue missions, environmental monitoring for pollution detection and estimation, target tracking, cooperative detection of hazardous materials in contaminated environments, forest fire monitoring, oceanographic modeling, etc. [1]–[4]. Each such application can in fact be cast as a problem of trying to estimate some unknown, spatially distributed target of interest given some *a priori* measurement. Despite these numerous applications and the potential of MSNs to resolve environmental mapping, the lack of (**Ram:** explain what is missing specifically now) has meant that such environmental mapping has relied predominantly on human-controlled efforts. This paper aims to develop a class of sensing and motion model for MSNs to autonomously and collectively obtain an accurate representation of an arbitrary spatial target map under the Bayesian framework.

As a motivating example, consider the following scenario: a team of unmanned vehicles is deployed to monitor the radiation levels over a region of interest. Each vehicle is equipped with a close-range noisy radiation sensor, to inspect the radiation level over the region of interest. The vehicles must approach the radiation sources close enough to ensure accurate measurement while collectively building a radiation map over the entire region. To perform the required mission,

the group of vehicles must solve two problems: (i) *deployment*: the vehicles must be able to distribute themselves to maximize the likelihood that their collective measurements can be effectively combined to estimate the true target distribution; and (ii) *map reconstruction*: robots must be able to effectively update their posterior map using the prior believe on the map and new observations retrieved at the current configuration. *The objective of this paper is to design an effective, cooperative deployment and map reconstruction strategy for the robotic network.* This focuses on a group of homogeneous mobile robots equipped with range sensors tasked with building a spatial distribution map of a bounded domain where the data and the spatial coordinates of the data are correlated (e.g., precipitation map, heat distribution, radiation map, etc). (**Ram:** describe in a single sentence how its done in this paper)

Bayesian inference has guided the development of a variety of tools to recursively estimate the state of a dynamical system and has as a result provided a powerful statistical tool to manage the measurement of uncertainties. In particular, during mobile robot search and exploration, the Bayesian method has enabled the construction of tools for the localization of targets [5], target tracking [6], POMDP planning [7], and source localization [8], [9] (e.g., aerosol, gas, sound, chemical plume, radiation sources). In this latter instance for example, the Bayesian approach led to the development of an autonomous search algorithm that maximized information gain to find a diffusive source [8] (**Ram:** why is this paper in particular relevant and what is the missing gap here between what they are proposing and what you are proposing in this paper??).

(**Ram:** this next paragraph needs to more clearly explain why their method (specifically the one in [10] is deficient. At the moment it seems like a nice method to solve the problem you are proposing.) While they used a non-Bayesian method, [10] is the most related work that deals with target distribution mapping—in their work, constructing concentration map—by a mobile robot where the mission is of both detection and identification of gas continuously distributed over a space. In [10], Lilienthal and Duckett observed that measurement from diffusive sensor provides information about a relatively smaller area compared to the measurement extracted from sonar, or laser range scans. To overcome the limitation, they proposed a novel grid-mapped technique which use Gaussian weighing kernel to model the decreasing likelihood that a particular reading represents the true concentration with respect to the distance from the point of measurement. Our study is motivated by the their work [10], multi-robot probabilistic

search for diffusive source [8], and the studies on popular multi-robot deployment problems [3]. While those studies [3] uses static, prior topological target distribution, and their goal is to find deployment policy maximizing the collective quantity of interest, e.g., Quality of Service (QoS), Signal-to-Noise Ratio (SNR) given the target distribution known *a priori*, our paper presents a general framework for incremental reconstruction of spatially distributed target information map over a bounded region using new measurements made from MSN, where sensors are dynamically reconfigured to maximize the most recent belief on the target distribution.

This paper's primary contributions are threefold: first, a probabilistic sensor model that incorporates joint target detection and spatial distribution estimation by a group of mobile sensors while capturing a key characteristic of the target detection task—the probability of seeing a target, monotonically decreases as a function of the distance between the sensor and the target, which is atypical of range sensors (**Ram: I don't understand what you mean by: atypical of range sensors.**). Second, a class of deployment strategies ranging from decentralized to fully coordinated ones where each control law is designed to maximize the observation likelihood marginalized over the previous belief of the target distribution. Finally, a variation of the Sequential Importance Resampling (SIR) Particle Filter which uses the joint observations and the updated configuration of the robots to update the posterior belief on the target by approximation.

Organizations: The rest of the paper is organized as follows. Section II presents notation used in the remainder of the paper, formally defines the problem of interest, and reviews a recursive Bayesian filter tailored to the problem. Section III presents a probabilistic sensor model. Section III studies the partitioned based approach to deployment, and the modified version of the sensor model discussed in Section IV. The deployment strategy is formally presented in Section V. Section VI discusses an approximate belief update method via particle filters. The effectiveness of this deployment and belief update approach is evaluated via simulation and real-world experimentation in Sections VII and VIII, respectively. Finally, Section IX concludes the paper and proposes a number of future directions.

II. METHOD FOR PROBABILISTIC MAPPING

This section presents the notation used throughout the paper, the problem of interest, and the recursive Bayesian filter.

A. Notations and Our System Definition

Throughout the text, the italic bold font is used to describe random quantities, a subscript t indicates that the value is measured at time step t , and \mathbb{Z}^+ denotes nonnegative integers. Given a continuous random variable x , if it is distributed according to a Probability Density Function (PDF), we denote it by f_x . Given a discrete random variable y , if it is distributed according to a Probability Mass Function (PMF), we denote it by p_y . Consider a group of m mobile robots deployed in a workspace, i.e., ambient space, $\mathcal{Q} \subseteq \mathbb{R}^d$. This paper assumes

$d = 1, 2, 3$ though the presented framework generalizes. Let $\mathbb{S} = \{(x, y) \in \mathbb{R}^2 \mid x^2 + y^2 = 1\}$ be a *circle*, then the state of m robots is the set of locations and orientations at time t , and it is represented as an m -tuple $x_t = (x_t^1, \dots, x_t^m)$, where $x_t^i \in \mathcal{Q} \times \mathbb{S}$. We denote by the set $x_{0:t} := \{x_0, \dots, x_t\}$ the robot states up to time t . Given a pair of states (x_t, x_{t+1}) , robots follow a way-point-based, continuous-time, deterministic motion model with dynamic constraints:

$$\dot{x}(t) = f(x(t), u(t)) \quad (1)$$

with boundary conditions $x(t_0) = x_t$ and $x(t_f) = x_{t+1}$ where u is a control, t_0 is the *initial time*, and t_f is the *final time* which is free.

Let π_t be the *optimal control policy*¹ which drives robots' state from x_t to x_{t+1} in minimum time under the dynamic (or kinematic) constraints. We define a *target* to be a physical object or some measurable quantity spatially distributed over a bounded domain. Let z be the *target state* which is a random vector. The target state consists of location, $q \in \mathcal{Q}$, and information states (quantitative information about the target), $I \in \mathcal{I} \subseteq \mathbb{R}^n$. The Cartesian product $\mathcal{Z} = \mathcal{Q} \times \mathcal{I}$ is the *target state space*. Let the m -tuple $y_t = (y_t^1, \dots, y_t^m)$ be the observations recorded by m robots at time step t where y_t^i denotes the observation made by the i^{th} sensor, and let the set $y_{1:t} := \{y_1, \dots, y_t\}$ denote observations made by m robots up to time t . (**Ram: it may make sense for the subsequent development for you to mention that y is a function of z and x .**) Note that if target location is unknown, observations made by different sensors are conditionally independent given the target location (**Ram: this is missing a citation**). (**Ram: it may also make sense for you to consider a simple example here just to formalize the notation for the reader**)

B. Problem Definition

Let b_t represent a *belief*, the posterior probability distribution over the target state space at time $t \in \mathbb{Z}^+$ (**Ram: Is $b_t = p(z \mid x_{0:t}, y_{0:t}, b_0)$**). Each belief depends on initial belief, b_0 , the set of robot configurations, $x_{0:t}$, and observations up to this point, $y_{1:t-1}$. The state of robots are assumed completely *known*. Let b^* be the *true posterior belief*² on the target state. Then for each $t \in \mathbb{N}$, given the initial belief, b_0 , our objective is obtain the sequence of optimal control policies (π_1, π_2, \dots) , each solves

$$\pi_t = \arg \max b_t, \quad t = 1, 2, \dots, \quad (2)$$

where each optimal policy between two time steps $[t, t+1)$, namely, π_t is subject to the dynamic constraints given in (1). To this end, we quantify the difference between the true posterior belief, b^* and an approximation using our method via the Kullback-Leibler (K-L) divergence. We demonstrate via our numerical simulation in Section VII that for a given $\epsilon > 0$, there is a dynamically varied stopping time $T > 0$ such

¹An example of such an optimal control could be the Linear-Quadratic Regulator if the dynamics were linear.

²We assume for now that the true posterior target distribution can be obtained, e.g., via exhaustive search and measurements made by a MSN.

that by the sequence of optimal policies, (π_1, \dots, π_T) , $t > T$ implies $D_{\text{KL}}(b_t \| b^*) < \epsilon$. **(Ram: How do you in practice solve this problem since we do not know b_t^* ?)**

C. Recursive Bayesian Filter

We present an overview of the Bayesian filter, and the derivation of the filtering equations for our primary goal: spatial distribution mapping by m robots. We denote the belief about a given target state z at time $t \in \mathbb{N}$ as $b_t(z)$, and the belief of target information state I given the target located at q is given by:

$$b_t(I | q = q) = f_{I|b_0, x_{0:t}, y_{1:t}, q}(I | b_0, x_{0:t}, y_{1:t}, q) \quad (3)$$

where we denote the initial belief on target state by b_0 . If the probability distribution about the target location, namely f_q is known *a priori*, the belief on the complete target state z is:

$$\begin{aligned} b_t(z) &= f_{z|b_0(z), x_{0:t}, y_{1:t}}(z | b_0(z), x_{0:t}, y_{1:t}) \\ &= b_t(I | q = q) f_q(q). \end{aligned} \quad (4)$$

(Ram: I don't understand the marginal in the first line of the previous equation. Are you saying that we know b_0 or $b_0(z)$? Those are two distinct objects.) If there is no prior knowledge of the target information at the initial time, one can choose the prior distribution as the *uniform* density. Recall that the generic Bayes' Theorem states, $P(B | A) = \frac{P(A|B)P(B)}{P(A)}$ where A, B are events, $P(B | A)$ is the posterior probability distribution, $P(A | B)$ is the likelihood function, $P(B)$ is the prior probability distribution, and $P(A)$ is the marginal probability of the event A . Let the event B represent the prior belief on target information state $b_{t-1}(I | q = q)$, and A represent the sensor measurements at time t , y_t , then applying *Bayes' theorem*, (3) becomes

$$\begin{aligned} b_t(I | q = q) &= \frac{f_{y_t|z, b_0(z), x_{0:t}, y_{1:t-1}}(y_t | z, b_0(z), x_{0:t}, y_{1:t-1}) b_{t-1}(I | q = q)}{f_{y_t|q, b_0(z), x_{0:t}, y_{1:t-1}}(y_t | q, b_0(z), x_{0:t}, y_{1:t-1})} \end{aligned}$$

where $t \in \mathbb{N}$ **(Ram: I still do not understand this previous equation. Here are my questions: 1) is it $b_0(z)$ or b_0 2) is it $x_{0:t}$ or $x_{0:t-1}$?)**. Due to our sensor model (this is discussed in the next section), the observation y_t is conditionally independent on z and x_t **(Ram: again is this supposed to be $b_0(z)$ or b_0 ?)**. One can simplify the likelihood function in the target information map by using this observation, which yields:

$$b_t(I | q = q) = \eta_t f_{y_t|z, x_t}(y_t | z, x_t) b_{t-1}(I | q = q) \quad (5)$$

where

$$\eta_t := \left(f_{y_t|q, b_0(z), x_{0:t}, y_{1:t-1}}(y_t | q, b_0(z), x_{0:t}, y_{1:t-1}) \right)^{-1}$$

denotes the marginal probability, which is known as the *normalization constant*. This usually cannot be directly computed, but can be obtained by utilizing the total law of probability:

$$\eta_t = \left(\int_{\mathcal{I}} f_{y_t|z, x_t}(y_t | z, x_t) b_{t-1}(I | q = q) dI \right)^{-1} \quad (6)$$

By joining the (4) and (5), one can obtain a simplified form of the filtering equation:

$$b_t(z) = \eta_t f_{y_t|z, x_t}(y_t | z, x_t) b_{t-1}(z) \quad (7)$$

$$= \left(\prod_{i=1}^t \eta_i f_{y_i|z, x_i}(y_i | z, x_i) \right) b_0(z). \quad (8)$$

We assume that m robots share their beliefs **(Ram: so you are assuming full information sharing?)**.

III. PROBABILISTIC RANGE SENSOR MODEL

Each mobile robot is equipped with a *range sensor* that can measure quantitative information from afar and a *radio* to communicate with other nodes to share its belief. Each range sensor measurement is corrupted by noise, and the measurement is valid only if the target is detected. This combined range sensor model joins the generic noisy sensor model with the binary sensor model [11]. In fact, this combined range sensor model has been experimentally validated during an object mapping and detection task using a laser scanner [12]. We postulate that this model is general enough to model other range sensors as well; as long as the sensor is capable of distinguishing the target from the environment, and has uniform sensing range. A few example sensors satisfying these characteristics are 360-degree camera, wireless antenna, Gaussmeter, heat sensor, olfactory receptor, etc.

During target detection, we assume each sensor returns a 0 if a target is detected or 1 otherwise. The ability to detect a target for each i^{th} robot is a random variable y_B^i with a distribution that depends on the relative distance between the target and robot. This binary detection model, however, does not account for false positive or negatives. The probability of the event that all m sensors with configuration x_t fail to detect the target located at $q \in \mathcal{Q}$:

$$p_{y_{B,t}|x_t, z}(y_{B,t} = \mathbf{0} | x_t, z = (q, I)) \quad (9)$$

$$= p_{y_{B,t}|x_t, q}(y_{B,t} = \mathbf{0} | x_t, q = q) \quad (10)$$

$$= \prod_{i=1}^m p_{y_{B,t}^i|x_t, q}(y_{B,t}^i = 0 | x_t, q = q) \quad (11)$$

where $\mathbf{0} = \underbrace{(0, \dots, 0)}_m$.

For measuring a quantity of interest from a given spatial distribution, we consider a generic, noisy sensor model, where each sensor reports information regarding the environment, such as intensity data, as a *vector of reals*. Let $y_I = (y_I^1, \dots, y_I^n)$ be a n -random tuple for the measurements where n is the dimension of the sensor input. Without loss of generality, we assume that each random variable y_I^i has *range* $[I_{\min}^i, I_{\max}^i]$ where, $I_{\min}^i, I_{\max}^i \in \mathbb{R}$ for all $i \in \{1, \dots, n\}$.

Let the random variable $y_t = (y_t^1, \dots, y_t^m)$ denote the *total observation* which is the collection of all observations reported by m sensors at time t , where each y_t^i is the Cartesian product of the two previously defined random vectors. Note that two

random vectors \mathbf{y}_B^i and \mathbf{y}_I^i are *independent*³ when conditioned on x_t, z so that joint PDF can be computed as:

$$f_{\mathbf{y}^i|z,x}(\mathbf{y}^i | z, x) = p_{\mathbf{y}_B^i|z,x}(\mathbf{y}_B^i = \mathbf{y}_B^i | z, x) f_{\mathbf{y}_I^i|z,x}(\mathbf{y}_I^i | z, x) \quad (12)$$

where $\mathbf{y}_B^i \in \{0, 1\}$. Since the set of observations $\mathbf{y}^1, \dots, \mathbf{y}^m$ are made independently by m sensors, the joint probability distribution by m sensors, given a target at z becomes:

$$f_{\mathbf{y}_t|x_t,z}(\mathbf{y}_t | x_t, z = z) = \prod_{i=1}^m f_{\mathbf{y}_t^i|x_t,z}(\mathbf{y}_t^i | x_t, z = z) \quad (13)$$

$$= \prod_{i=1}^m p_{\mathbf{y}_{B,t}^i|x_t,z}(\mathbf{y}_{B,t}^i = \mathbf{y}_{B,t}^i | x_t, z = z) \times \prod_{i=1}^m f_{\mathbf{y}_{I,t}^i|x_t,z}(\mathbf{y}_{I,t}^i | x_t, z = z) \quad (14)$$

$$= p_{\mathbf{y}_{B,t}|x_t,z}(\mathbf{y}_{B,t} = \mathbf{y}_{B,t} | x_t, z = z) \times f_{\mathbf{y}_{I,t}|x_t,z}(\mathbf{y}_{I,t} | x_t, z = z). \quad (15)$$

IV. PARTITION-BASED DEPLOYMENT APPROACH

Due to the limitation of the effective sensing range found on physical range sensors, we consider a partitioned-based strategy where the workspace is partitioned into m disjoint regions, and each robot is assigned to a region where it confines its detections (**Ram: just to be clear we are only going to consider the fully partitioned strategy in this paper?**). This so called partitioned-based strategy is common to multi-robot coverage problems [3], [13]–[15]. The most popular one is based on the Voronoi tessellations (see e.g., [3], which we call a *non-coordinated strategy*). There are, in fact more general methods, which partition the workspace into p regions and assign $k \in [2, m]$ robots each region (note that if $k = m$, the method becomes *centralized*) [13]. By doing so, one can ensure that each target has a chance to be detected by at least one of the k sensors. This approach, which we call the *coordinated strategy*, can provide relative robustness by varying the value of k from 1 to m . Thus, if each sensor has an effective sensing range long enough to cover the whole workspace, utilizing all m sensors to detect every target in the workspace becomes the most desirable strategy.

A. The Optimal Partition

Consider m sensors and a workspace partition of \mathcal{Q} into l disjoint regions, W such that $W = (W_1, \dots, W_l)$, where $\cup_i W_i = \mathcal{Q}$, and $W_i \cap W_j = \emptyset$ for all i, j pairs with $i \neq j$. Suppose the target location is a random variable z with PDF $\phi : \mathcal{Q} \rightarrow \mathbb{R}_{\geq 0}$. For a given target $z \in \mathcal{Q}$, we define the probability that a sensor located at x fails to detect target, using a real-valued function $h(\|z - x_i\|)$ as a probability measure (**Ram: h is a function $h(\|z - x_i\|)$ is a number; moreover**

³This assessment is based on the underlying assumption that the detection event and sensor measurement event are independent to each other (**Ram: is this a valid assumption?**).

do you mean that h is the pdf?)⁴, which is assumed to decrease monotonically as a function of the distance between the target and the i^{th} sensor. Consider a bijection kG that maps a region to a set of k -points where the pre-superscript k explicitly states that the region is mapped to exactly k points. Additionally we make the following definitions:

Definition 4.1 (An Order- k Voronoi Partition [16]). *Let x be a set of m distinct points in $\mathcal{Q} \subseteq \mathbb{R}^d$. The order- k Voronoi partition of \mathcal{Q} based on x is the collection of regions that partitions \mathcal{Q} where each region is associated with the k nearest points in x .*

We also define another bijection ${}^kG^*$ that maps a region to a set of k nearest points (**Ram: what set of points?**). The total probability that all m sensors fail to detect a target drawn by a distribution ϕ from \mathcal{Q} is:

$$\int_{\mathcal{Q}} p_{\mathbf{y}_B|x,q}(\mathbf{y} = \mathbf{0} | x, q = q) \phi(q) dq. \quad (16)$$

By substituting \mathcal{Q} with the workspace partition W , and $p_{\mathbf{y}_B|x,q}(\mathbf{y} = \mathbf{0} | x, q = q)$ with likelihood function h , we have

$$H(x, W, {}^kG) = \sum_{j=1}^l \int_{W_j} \left(\prod_{x_i \in {}^kG(W_j)} (1 - h(\|q - x_i\|)) \right) \phi(q) dq \quad (17)$$

where we note again that the joint missed-detection events are conditionally independent, if conditioned on x . In fact, the order- k diagram (**Ram: what is a diagram?**) is the optimal workspace partition which minimizes H for each choice of x and k :

Theorem 4.1 ([15]). *For a given x and k , $H(x, {}^kV, {}^kG^*) \leq H(x, W, {}^kG)$ for all $W, {}^kG$.*

Note that the order- k Voronoi partition V_k , along with the map G_k^* are uniquely determined given x , ϕ , and \mathcal{Q} .

B. Partitioned Range-limited Sensor Model

This section presents a practical sensor model that is better suited to distributed target detection based on the order- k Voronoi partition. The modified sensor model is a combination of deterministic workspace partitioning method and the probabilistic sensor model presented in Section III. In addition, we introduce another constraint for the model, namely the *effective sensing range*, $r_{\text{eff}} > 0$, to take into account the fact that the noisy measurement taken by each sensor does not depend on its distance to the target, if the target is sufficiently close to the sensor⁵. For a given k , and $z = (q, I)$, we assume that the

⁴For the numerical simulations purpose, we further assume that $h(\cdot)$ is continuously differentiable function non-increasing on its domain, and the image of h must be in $[0, 1]$ for it to be a probability measure.

⁵Recall that in our proposed sensor model, we assumed two tasks, detection and measurement, to be completely decoupled, nevertheless our generic noisy sensor model—which which treats all measurements taken within its maximum sensor range equally—can also be generalized to other popular forms (e.g., Gaussian, radially non-uniform, anisotropic, etc.)

following is true for our new sensor model:

Positive detection likelihood:

$$p_{\mathbf{y}_{B,t}^i | \mathbf{z}, x_t}(\mathbf{y}_t^i = 1 | x_t, z) = \begin{cases} h(\|q - x_t^i\|) \times f_{\mathbf{y}_{I,t}^i | x_t, \mathbf{z}}(\mathbf{y}_{I,t}^i | x_t, z), & \text{if } q \in {}^k G_t^*(x_t^i) \cap \mathcal{B}(x_t^i, r_{\text{eff}}), \\ 0, & \text{otherwise,} \end{cases}$$

Negative detection likelihood:

$$p_{\mathbf{y}_{B,t}^i | \mathbf{z}, x_t}(\mathbf{y}_t^i = 0 | x_t, z) = \begin{cases} (1 - h(\|q - x_t^i\|)) \times f_{\mathbf{y}_{I,t}^i | x_t, \mathbf{z}}(\mathbf{y}_{I,t}^i | x_t, z), & \text{if } q \in {}^k G_t^*(x_t^i) \cap \mathcal{B}(x_t^i, r_{\text{eff}}), \\ 1, & \text{otherwise,} \end{cases} \quad (18)$$

where $\mathcal{B}(x, r)$ is an open ball with radius r centered at x .

V. DEPLOYMENT STRATEGY

As discussed in Section III, a measurement for a target is valid only if the target is detected. Thus, we consider a deployment strategy where robots move to locations maximizing their marginal likelihood of *positive* detections over the previous belief on the target state. Note that the marginal likelihood of positive detection is obtained by taking integrals on the positive likelihood estimate over the prior target distribution.

For $t \geq 2$ and sensors located at x_t , let l_t^+ be the positive likelihood that targets are detected by at least one sensor, then:

$$l_t^+(x_t) := \int_{\mathcal{Z}} p_{\mathbf{y}_{B,t-1} | x_t, \mathbf{z}}(\mathbf{y}_{B,t-1} \neq \mathbf{0} | x_t, z) \times f_{\mathbf{y}_{I,t-1} | x_t, \mathbf{z}}(\mathbf{y}_{I,t-1} | x_t, z) b_{t-2}(z) dz. \quad (19)$$

Similarly, let l_t^- be the negative likelihood that target are missed detected by m sensors which is:

$$l_t^-(x_t) := \int_{\mathcal{Z}} p_{\mathbf{y}_{B,t-1} | x_t, \mathbf{z}}(\mathbf{y}_{B,t-1} = \mathbf{0} | x_t, z) \times f_{\mathbf{y}_{I,t-1} | x_t, \mathbf{z}}(\mathbf{y}_{I,t-1} | x_t, z) b_{t-2}(z) dz. \quad (20)$$

We are interested in maximizing the likelihood of positive observation. Unfortunately, the integral term has a combinatorial number of terms, so it is impractical to compute (19) for large m . Instead we employ an alternative approach. First note the following:

Lemma 5.1. $\arg \min l_t^+(x_t) = \arg \min l_t^-(x_t)$

The proof of this lemma follows from the law of total probability and is omitted. According to Lemma 5.1, maximizing the likelihood that at least one sensor detects every target in the workspace, given the previous target belief, is identical to minimizing the likelihood that all m sensors fail to detect a target in \mathcal{Q} .

Let $x_t^* := \arg \min l_t^+(x_t) = \arg \min l_t^-(x_t)$, then:

$$x_t^* = \arg \min \left\{ \int_{\mathcal{Z}} p_{\mathbf{y}_{B,t-1} | x_t, \mathbf{q}}(\mathbf{y}_{B,t-1} = \mathbf{0} | x_t, z) \times p_{\mathbf{y}_{I,t-1}}(y_{I,t-1} | z) b_{t-2}(z) \right\} dz \quad (21)$$

$$= \arg \min \left\{ \int_{\mathcal{Q}} p_{\mathbf{y}_{B,t-1} | x_t, \mathbf{q}}(\mathbf{y}_{B,t-1} = \mathbf{0} | x_t, q) \times \int_{\mathcal{I}} p_{\mathbf{y}_{I,t-1} | \mathbf{z}}(y_{I,t-1} | z) b_{t-2}(z) dI dq \right\} \quad (22)$$

where the detection likelihood is conditionally independent on \mathbf{I} if conditioned on x and \mathbf{q} . We note that the maximum of the positive observation likelihood depends not only on the distance between targets and the robots, but also on the likelihood of the noisy sensor measurements. Thus, given the prior belief and the observations, robots find and move to new locations, and the posterior belief is updated at the new locations given the collected information. We define a new belief that joins the previous belief with the current measurement likelihood as:

$$\begin{aligned} \tilde{b}_{t-1}(q) &:= \int_{\mathcal{I}} p_{\mathbf{y}_{I,t-1} | \mathbf{z}}(y_{I,t-1} | z) b_{t-2}(z) dI \\ &= \underbrace{f_{\mathbf{q}}(q)}_{\text{PDF of } \mathbf{q}} \underbrace{\int_{\mathcal{I}} p_{\mathbf{y}_{I,t-1} | \mathbf{z}}(y_{I,t-1} | z) b_{t-2}(z) dI}_{\text{marginal likelihood of } \mathbf{y}_{I,t-1} \text{ conditioned on } q} dI, \end{aligned} \quad (23)$$

and a cost function

$$L(x_t, y_{t-1}, \tilde{b}_{t-1}) := \int_{\mathcal{Q}} p_{\mathbf{y}_{B,t-1} | x_t, \mathbf{q}}(\mathbf{y}_{B,t-1} = \mathbf{0} | x_t, q) \tilde{b}_{t-1}(q) dq \quad (24)$$

which illustrates the explicit dependence on the previous belief \tilde{b}_{t-1} and previous observations y_{t-1} . Then, our problem becomes

$$x_t^* = \arg \min_{x_t} L(x_t, y_{t-1}, \tilde{b}_{t-1}). \quad (25)$$

We note that for a given k , by substituting \tilde{b}_{t-1} , x_t , y_{t-1} with ϕ , x , y respectively, and plugging observation likelihood functions from (18) and (24) becomes identical to $H(x, W, G^k)$ which was previously defined in (17). If the perception model is differentiable, our deployment strategy can use the gradient: $\nabla_{x_t} L(x_t, y_{t-1}, \tilde{b}_{t-1})$ to find the desirable locations of the robots to maximize the observation likelihood as described in Algorithm 1. We use \hat{x}_t to denote the suboptimal solution obtained by the gradient algorithm at time t .

Theorem 5.1. *Algorithm 1 is convergent.*

The formal proof of Theorem 5.1 is similar to the proof contained in our previous paper [15], and is thus omitted.

VI. BELIEF APPROXIMATION BY PARTICLE FILTERING

We consider the Particle Filtering approach to reduce the complexity of the target map evolution (**Ram: how is the target map evolving? I thought it was fixed...?I think you**

Algorithm 1: Gradient Algorithm (MMLE)

Input: $L, x_{t-1}, \epsilon > 0, \tilde{b}_{t-1}, y_{t-1}$
Output: \hat{x}_t
 $k \leftarrow 0, x_{t,k} \leftarrow x_{t-1}, \delta L \leftarrow \epsilon$
while $\delta L > \epsilon$ **do**
 foreach $i \in \{1, \dots, m\}$ **do**
 $x_{t,k+1}^i \leftarrow x_{t,k}^i - \alpha_{t,k}^i \nabla_{x_t^i} L(x_t, y_{t-1}, \tilde{b}_{t-1})$
 // $\alpha_{t,k}^i$ is obtained using a line search method
 $\delta L \leftarrow L(x_{t,k}, y_{t-1}, \tilde{b}_{t-1}) - L(x_{t,k+1}, y_{t-1}, \tilde{b}_{t-1})$
 $k \leftarrow k + 1$
return $\hat{x}_t \leftarrow x_{t,k}$

mean the reconstruction is being updated as observations appear...).

A. Low Discrepancy Sampling

For our numerical simulations, we consider a low discrepancy sampling method (e.g., Halton-Hammersley sequence [17]) to sample continuously distributed targets in $z \in \mathcal{Z} = \mathcal{Q} \times I$. This approach has been used for sampling-based algorithms for robot motion planning [18].

B. SIR Particle Filter

We consider Sequential Importance Resampling (SIR) [19] for the particle filtering process. For a given distribution on target locations, $f_q(q)$, at each time t , based on the observations, the locations belief hypothesis is populated for N_1 samples initially generated with Halton-Hammersley sequence.

$$\left\{ (q_t^1, \tilde{w}_{T,t}^1), \dots, (q_t^{N_1}, \tilde{w}_{T,t}^{N_1}) \right\} \quad (26)$$

where for each $i \in \{1, \dots, N_1\}$,

$$\tilde{w}_t^i = p_{y_{B,t}|\hat{x}_t, z}(y_{B,t} | \hat{x}_t, z = (q_t^i, I)) \quad (27)$$

for all $I \in \mathcal{I}$. In a similar manner, for each sample q_t^i the information belief hypothesis is populated for N_2 samples from \mathcal{I} initially generated by the Halton-Hammersley sequence:

$$\left\{ (I_t^{i1}, \tilde{w}_{I,t}^{i1}), \dots, (I_t^{iN_2}, \tilde{w}_{I,t}^{iN_2}) \right\} \quad (28)$$

where for each $i = 1, \dots, N_1$, $\sum_{j=1}^{N_2} w_{I,t}^{ij} = 1$, and

$$\tilde{w}_{I,t}^{ij} \propto p_{y_{I,t}|\hat{x}_t, z}(y_{I,t} | \hat{x}_t, z = (q^i, I^{ij})) \quad (29)$$

for all $i \in \{1, \dots, N_1\}$. If we let $z^{ij} := (q^i, I^{ij})$ and $\tilde{w}_t^{ij} := \tilde{w}_{T,t}^i \tilde{w}_{I,t}^{ij}$ then the final expression for the set of $N := N_1 N_2$ particle-weight pairs at time t is

$$\left\{ \left\{ (z^{ij}, \tilde{w}_t^{ij}) \right\}_{j=1}^{N_2} \right\}_{i=1}^{N_1} = \{z^k, \tilde{w}_t^k\}_{k=1}^N \quad (30)$$

After resampling and normalizing, the approximate posterior belief becomes

$$\hat{b}_t(z) = \sum_{k=1}^N w_t^k \delta(z_t - z_t^k) \quad (31)$$

which is a form of discrete random measure where the w_t^1, \dots, w_t^N are resampled, normalized weight such that $\sum_{k=1}^N w_t^k = 1$, and $\delta(z_t - z_t^k)$ is Dirac-delta function evaluate at z_t^k . We note that resampling is only taken on the target information state, namely, I_t . The whole filtering process is depicted in Algorithm 2. Note that as discussed in previous studies [20], our particle filter uses standard re-sampling scheme to ensure the convergence of the mean square error toward zero with a convergence rate of $1/N_2$ for all $q \in \mathcal{Q}$.

Algorithm 2: Filtering Algorithm

Input: $\hat{b}_{t-1} = \{z^l, w_{t-1}^l\}_{l=1}^N = \{\{(q^i, I^{ij}), w_{B,t-1}^i w_{I,t-1}^{ij}\}_{j=1}^{N_2}\}_{i=1}^{N_1}, y_{t-1}, y_t, \hat{x}_{t-1}$
Output: \hat{b}_t
// Propagate motion model using MMLE (maximum marginal likelihood estimation); see Algorithm 1
 $\hat{x}_t \leftarrow \text{MMLE}(\hat{b}_{t-1}, y_{t-1}, \hat{x}_{t-1})$
// SIR Particle Filter
// 1) Update using the observation model
foreach $i \in \{1, \dots, N_1\}$ **do**
 $\tilde{w}_{B,t}^i \leftarrow p_{y_{B,t}|\hat{x}_t, q}(y_{B,t} | \hat{x}_t, q = q_t^i)$
 foreach $j \in \{1, \dots, N_2\}$ **do**
 $\tilde{w}_{I,t}^{ij} \leftarrow p_{y_{I,t}|\hat{x}_t, z}(y_{I,t} | \hat{x}_t, z = (q^i, I^{ij}))$
// 2) Resample and Normalize
 $\{w_t^l\}_{l=1}^N \leftarrow \text{Resample}(\{\tilde{w}_t^l\}_{l=1}^N, \{w_{t-1}^l\}_{l=1}^N)$
return $\hat{b}_t \leftarrow \{z^l, w_t^l\}_{l=1}^N$
// Low Variance Resampling [21]
function $\text{Resample}(\{\tilde{w}_t^l\}_{l=1}^N, \{w_{t-1}^l\}_{l=1}^N)$
 forall the $i \in \{1, \dots, N_1\}, j \in \{1, \dots, N_2\}$ **do**
 $\bar{w}_{I,t}^{ij} \leftarrow \frac{\tilde{w}_{I,t}^{ij} \cdot w_{I,t-1}^{ij}}{\sum_{i=1}^{N_1} \sum_{j=1}^{N_2} \tilde{w}_{I,t}^{ij} \cdot w_{I,t-1}^{ij}}$
 foreach $i \in \{1, \dots, N_1\}$ **do**
 $\delta \leftarrow \text{rand}((0; N_2^{-1}))$
 $\text{cdf} \leftarrow 0, k \leftarrow 0, c_j \leftarrow []$ for all j
 for $j = 0, j < N_2$ **do**
 $u \leftarrow \delta + j \cdot N_2^{-1}$
 while $u > \text{cdf}$ **do**
 $k \leftarrow k + 1$
 $\text{cdf} \leftarrow \text{cdf} + \bar{w}_{I,t}^{ik}$
 $c_{j+1} \leftarrow k$
 for $j = 1; j \leq N_2$ **do**
 $w_{I,t}^{ij} \leftarrow \frac{c_j}{N_2}$
 return $\{\{w_{B,t}^i \cdot w_{I,t}^{ij}\}_{j=1}^{N_2}\}_{i=1}^{N_1}$

VII. NUMERICAL SIMULATIONS

In this section, we present a suite of multi-agent deployment-map updating simulations with different sensor models.

Gaussian PDFs for the Observation Likelihood: For the simulation, we consider Gaussian kernels for the probability distributions of both the perception model, and the detection model. First, consider the conditional probability distribution

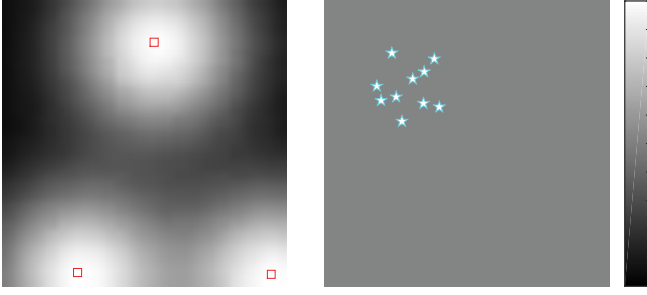


Fig. 1: Left: the expected target intensity (the ground truth), right: initial configuration of 10 robots where background color (gray) shows spatial density for every target is uniform. Squares in the left are the peaks of the mixture of Gaussians, and stars on the right are the robots' locations

for detection likelihood, positive and negative functions respectively

$$\begin{aligned} p_{\mathbf{y}_{B,t}^i | x_t, \mathbf{q}}(\mathbf{y}_{B,t}^i = 1 \mid x_t, \mathbf{q} = q) &= \eta_B \mathcal{N}(q, x_t^i, \Sigma_B) \\ &= \eta_B \frac{1}{2\pi |\Sigma_B|} \exp\left(-\frac{(q - x_t^i)^\top \Sigma_B^{-1} (q - x_t^i)}{2}\right), \end{aligned}$$

and

$$p_{\mathbf{y}_{B,t}^i | x_t, \mathbf{q}}(\mathbf{y}_{B,t}^i = 0 \mid x_t, \mathbf{q} = q) = 1 - \eta_B \mathcal{N}(q, x_t^i, \Sigma_B)$$

where $\mathcal{N}(q, x_t^i, \Sigma_B)$ is multivariate Gaussian with mean x_t^i and covariance matrix Σ_B , and η_B is a constant. Assume that the noisy sensor model is also a multi-variate Gaussian with mean $y_{I,t}^i$ and covariance matrix Σ_I .

$$f_{\mathbf{y}_{I,t}^i | x_t, \mathbf{I}}(y_{I,t}^i \mid x_t, \mathbf{I} = I) = \eta_I \mathcal{N}(I, y_{I,t}^i, \Sigma_I)$$

where η_I is normalization constant. The total observation likelihood is given by

$$\begin{aligned} f_{\mathbf{y}_{B,t}^i | x_t, \mathbf{z}}(y_{B,t}^i, y_{I,t}^i \mid x_t, \mathbf{z} = (q, I)) \\ = \begin{cases} \eta_B \eta_I (1 - \mathcal{N}(q, x_t^i, \Sigma_B)) \mathcal{N}(I, y_{I,t}^i, \Sigma_I), & \text{if } y_{B,t}^i = 0 \\ \eta_B \eta_I \mathcal{N}(q, x_t^i, \Sigma_B) \mathcal{N}(I, y_{I,t}^i, \Sigma_I), & \text{if } y_{B,t}^i = 1 \end{cases} \end{aligned}$$

Simulation settings: In the simulation, we consider \mathcal{Q} be a unit square space $[0, 1] \times [0, 1]$ in \mathbb{R}^2 , $\mathcal{I} = [0, 1]$, and $r_{\text{eff}} = \text{diam}(\mathcal{Q}) = \sqrt{2}$ (relaxed). Targets are uniformly distributed over \mathcal{Q} , and the initial expected spatial density of the target over \mathcal{Q} is given in Fig. 1 (left) as a mixture of Gaussian kernels. The intensity of the expected spatial distribution ranges from 0 to 1, which corresponds to black to white colored areas, respectively. The empty square denotes the peak of each kernel. As shown in Fig. 1 (right), at time 0, 10 mobile robots are deployed at the upper-left corner of \mathcal{Q} where the empty star denotes the robots' positions. We assume that there is no prior knowledge of the target information such that color intensity is also uniformly set to 0.5 out of 1. A number of particles used for the SIR filter is $N = N_1 \times N_2 = 1000 \times 100$. The value of the equipped noisy sensor's covariance matrix is fixed at $\Sigma_I = 0.5\mathbf{I}$, and the binary sensor's covariance will be varied.

Convergence of deployment algorithm: First, the behavior of

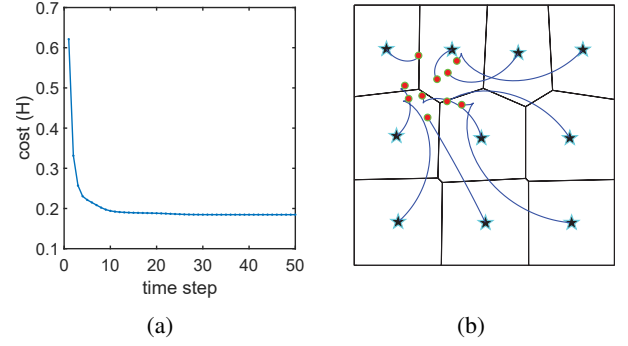


Fig. 2: One-time deployment, (a) cost change during Algorithm 1, (b) optimal path respecting unicycle kinematic constraint (small circles: initial positions, stars: target positions, solid lines: partitions at target positions)

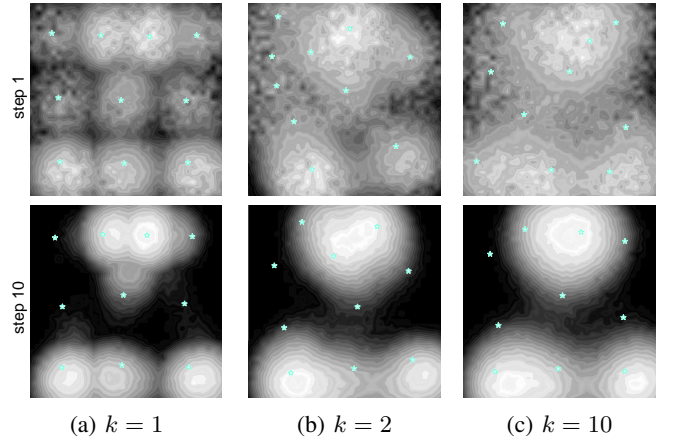


Fig. 3: Belief propagation using various methods with moderate detection range where $\Sigma_B = 0.04\mathbf{I}$ ((a) $k = 1$, (b) $k = 2$, (c) $k = 10$, the 1st row: step 1, the 2nd row: step 10, stars: positions of robots at 10th step)

the deployment strategy is discussed. Given the initial uniform prior belief, robots is governed by the gradient descent strategy (Algorithm 1) to obtain the next way-point x_1 for the next time step 1. As previously noted in the Section V, robots move toward the locations which maximize the likelihood of positive detections. Fig. 2(a) shows the convergence of the algorithm, and Fig. 2(b) illustrates the path generated by optimal control low when each robot has unicycle kinematics.

Filtering performance: Next, we present the evolution of the object map given the uniform, initial map (Fig. 1(right)) with successive positive observations, each followed by the gradient descent strategy and filtering process. Fig. 3 illustrates the map building process, by different methods with $k = 1, 2, 10$ respectively, given a moderate covariance values $\Sigma_B = 0.04\mathbf{I}$ for the binary detection where $\mathbf{I} \in \mathbb{R}^{d \times d}$ is an identity matrix, by showing robots' positions and the current belief at time step 1 and 10 respectively. The results in figures clearly show that the coordinated strategies ($k = 2, 10$) yields relatively better mapping results than non-coordinated strategy $k = 1$ compared to the ground truth map shown in Fig 1(left). In addition, Fig. 4 compares the K-L divergence values between different strategies during the evolution. Fig.

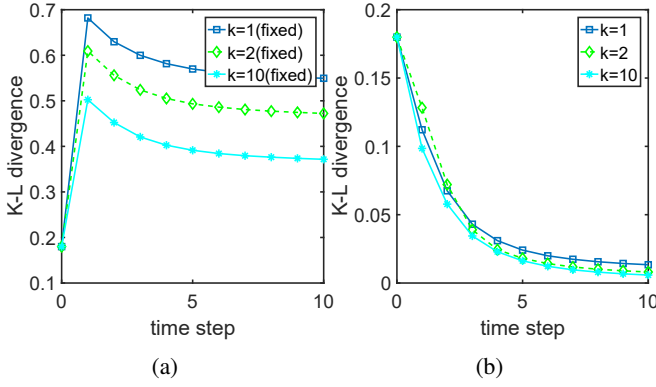


Fig. 4: Comparison of K-L divergence from the actual distribution between different sensor models during belief propagation; (a) robots are stationary, (b) robots are deployed via gradient algorithm

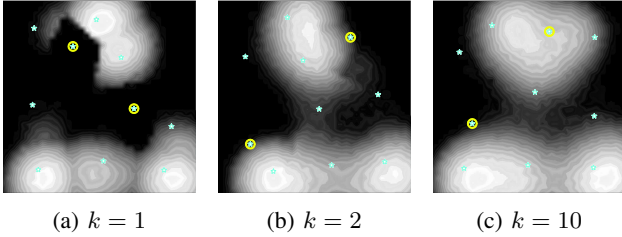


Fig. 5: Comparison of robots' configuration and beliefs at the final step with two approaches, $k = 1, 2, 10$ when two of the sensors fails (circled) and $\Sigma_B = 0.04I$ for both cases

4 also includes the case when robots are stationary⁶ merely to illustrate the pure filtering performance. As can be seen, our deployment strategy has noticeably improved the quality of the map retrieval for all cases. The occurrence of sudden jumps (between the time step 0 and 1) in the K-L divergence values observed in Fig 4(a) demonstrates the cases when the initial uniform density happened to a better ‘guess’ than the crude belief obtained after a single propagation of the filtering process.

Robustness to sensor failure: As seen in the previous

⁶The robots do not change their positions over time, and simply collect observations from the initial locations (as depicted in Fig. 1(right)).

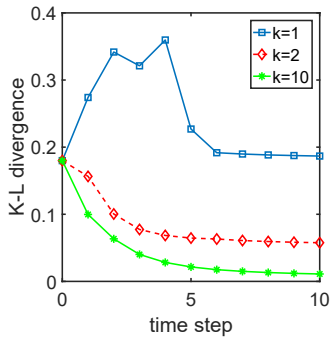


Fig. 6: Comparison of K-L divergence from the ground-truth distribution between multiple strategies ($k = 1, 2, 10$), when two sensors fail, during the evolution

section, the performance gain by the coordinated methods over the non-coordinated method ($k = 1$) is not large enough to trade-off the increased sensing cost. This section presents an example when the coordinated strategy becomes more desirable. And, this happens when the sensors are not perfect and likely to fail to detect a target. Results for configurations and spatial distributions after 10th step with $k = 1, 2, 10$, are shown in Fig. 5(a)-(c), respectively. As can be seen from Fig 5 and Fig. 6, the map retrieved by the coordinated strategies $k = 2, 10$ are more accurate, and more robust to the sensor failure compared to that obtained with the non-coordinated strategy. Due to its fully decentralized nature of the sensor model, it is not surprising to see from this example that the non-coordinated method works poorly under the sensor failures.

VIII. AN EXAMPLE: PRECIPITATION MAPPING USING WINDSHIELD WIPER DATA

Existing methods for precipitation measurements (e.g., weather radar, stationary rain gauges, etc) usually do not pose high enough temporal resolution for building a precipitation map to be used for time critical hydrological applications, such as, urban flash floods monitoring. In this section, we provide an example based on real-world data which shows that our Bayesian update scheme can be used for online precipitation mapping via utilizing the multi-vehicles' real-time windshield wiper data, which is spatially precise, and has much higher temporal resolution than the data collected from other sources. The vehicle wiper dataset—obtained from the University of Michigan Transportation Research Institute (UMTRI)—contains vehicle locations along with their wiper intensity data (four normalized intensity modes: 0, 0.33, 0.66, 1) which is generated at every 2ms. The windshield wiper data is collected from up to 69 vehicles. We consider a rainfall event occurred at the city of Ann Arbor between 21:47 and 22:26 on August 11th in 2014 (in UTC time). As shown in Fig 7, the rectangular area, $[-83.8, -83.66] \times [42.22, 42.34]$ (longitude, latitude in GPS coordinates, respectively) contains the boundary of Ann Arbor, which is drawn by lines. We assume that driver in each vehicle turns on the windshield wiper when detecting rain, and turns it off, otherwise, immediately in both cases. In addition, each driver is assumed to be capable of detecting rain from up to 1 mile away from the source of rain (i.e., $r_{\text{eff}} = 1$). We consider a product of two Gaussians—one with covariance matrices I (unit: mile) for detection, and the other with $0.5I$ (unit: normalized wiper intensity) for the intensity measurement, respectively—as the windshield wiper sensor model. Since, we did not have control over the vehicles at the time, the map is updated merely using the passively gathered windshield wiper measurements without utilizing our deployment algorithm, namely, Algorithm 1. For our algorithm, the initial expected wind wiper intensity is uniformly set to 0.3 out of 1 over the whole region. Fig 7 shows two time series of precipitation maps generated by the two different methods where the wiper data is sampled at every 1 second, and the radar is sampled at every 5 minute.

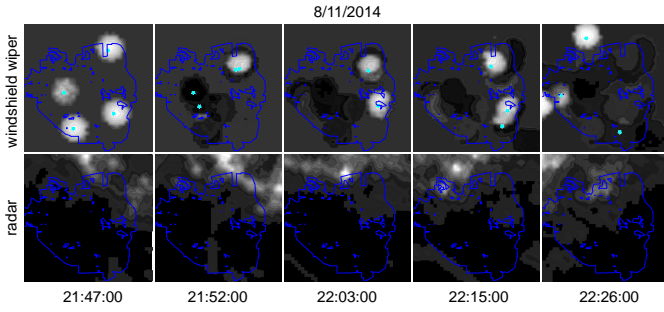


Fig. 7: A time series of precipitation map build by windshield wiper data collected from up to 4 vehicles using our Bayesian estimator (top row) vs a time series of map built by instantaneous precipitation rate measurements from NEXRAD-III (bottom row). Both maps are generated over the city of Ann Arbor, MI, USA (lines: boundary of the city, stars: vehicles' locations, color intensity: relative precipitation rate where the maximum precipitation rate by the radar is 2in/hr)

The 1st row of Fig. 7 shows incremental mapping by our method (non-coordinated strategy, $k = 1$). The color intensity shows the relative windshield wiper intensity where brighter area implies relatively more precipitation, and the black area means no precipitation⁷. The figures shown in the 2nd row of Fig. 7 illustrates the instantaneous precipitation rate measured by the NOAA Next Generation Radar Level III (NEXRAD-III). The radar is a Doppler type which is located at Detroit, the nearest NOAA's station to the city of Ann Arbor.

The rough visual correlation that is shown between the two series of maps shown in Fig 7, especially at the later time (22:26:00) is, unfortunately, not sufficient to validate the real-world performance of our method. There can be numerous reasons for the dissimilarity between the two. In the following, we will discuss a few of them briefly. First, weather radar observations are known to frequently provide unreliable information, e.g., due to blocking or deflection of radar beam, non-precipitation echo (see, e.g., [22] to find more details on this topic). In other words, the radar measurements are not consistent enough to be used as the ground truth precipitation data. Second, relative to the size of the region of interest, the number of vehicle (only up to 4 vehicles were active during the rainfall event shown in this example) is not large enough to capture the spatial rainfall distribution reasonably well. Lastly, our assumption on the effective sensor range for drivers could have been either too restrictive or unrealistic.

IX. CONCLUSIONS AND FUTURE WORK

In this paper, we have presented a general deployment strategy for a fleet of autonomous vehicles for maximum recovery of spatial distribution map over a bounded space. It is expected that our method will fail if there are not enough number of mobile agents having long enough effective sensing ranges relative to the workspace size. One of our future works is, therefore, to develop multi-agent patrolling

⁷We have experimentally validated that there are very strong correlation between windshield wiper intensity and the actual precipitation rate by comparing the windshield wiper data and visual data from the in-vehicle mounted camera.

algorithms (see e.g., [23]) to compensate such problems where there are not enough number of sensors to cover the whole target space. Also, as reported in the literature [12], our combined sensor model can be used to model the real-world laser scanner's behavior, nevertheless, it is one of our future works to conduct extensive real world multi-robot experiments for further validation of our range sensor model. Lastly, we assumed in this study that the beliefs are shared between robots such that both tasks of propagating and approximating belief require a central entity. It is one of our future works to devise distributed communication protocol to enable distributed belief estimation.

REFERENCES

- [1] S. S. Dhillon and K. Chakrabarty, "Sensor placement for effective coverage and surveillance in distributed sensor networks," in *Wireless Communications and Networking*, 2003. WCNC 2003. 2003 IEEE, vol. 3. IEEE, 2003, pp. 1609–1614.
- [2] A. Howard, M. J. Mataric, and G. S. Sukhatme, "Mobile sensor network deployment using potential fields: A distributed, scalable solution to the area coverage problem," in *Distributed autonomous robotic systems 5*. Springer, 2002, pp. 299–308.
- [3] J. Cortés, S. Martínez, T. Karatas, and F. Bullo, "Coverage control for mobile sensing networks," *Robotics and Automation, IEEE Transactions on*, vol. 20, no. 2, p. 243255, 2004.
- [4] L. Yu, N. Wang, and X. Meng, "Real-time forest fire detection with wireless sensor networks," in *Wireless Communications, Networking and Mobile Computing, 2005. Proceedings. 2005 International Conference on*, vol. 2. IEEE, 2005, pp. 1214–1217.
- [5] F. Bourgault, T. Furukawa, and H. F. Durrant-Whyte, "Coordinated decentralized search for a lost target in a bayesian world," in *Intelligent Robots and Systems, 2003.(IROS 2003). Proceedings. 2003 IEEE/RSJ International Conference on*, vol. 1. IEEE, 2003, pp. 48–53.
- [6] L. D. Stone, R. L. Streit, T. L. Corwin, and K. L. Bell, *Bayesian multiple target tracking*. Artech House, 2013.
- [7] S. Candido, J. Davidson, and S. Hutchinson, "Exploiting domain knowledge in planning for uncertain robot systems modeled as pomdps," in *Robotics and Automation (ICRA), 2010 IEEE International Conference on*. IEEE, 2010, pp. 3596–3603.
- [8] B. Ristic, M. Morelande, and A. Gunatillaka, "Information driven search for point sources of gamma radiation," *Signal Processing*, vol. 90, no. 4, pp. 1225–1239, 2010.
- [9] J.-M. Valin, F. Michaud, and J. Rouat, "Robust localization and tracking of simultaneous moving sound sources using beamforming and particle filtering," *Robotics and Autonomous Systems*, vol. 55, no. 3, pp. 216–228, 2007.
- [10] A. J. Lilienthal, M. Reggente, M. Trincavelli, J. L. Blanco, and J. Gonzalez, "A statistical approach to gas distribution modelling with mobile robots-the kernel dm+ v algorithm," in *Intelligent Robots and Systems, 2009. IROS 2009. IEEE/RSJ International Conference on*. IEEE, 2009, pp. 570–576.
- [11] P. M. Djuric, M. Vemula, and M. F. Bugallo, "Target tracking by particle filtering in binary sensor networks," *IEEE Transactions on Signal Processing*, vol. 56, no. 6, pp. 2229–2238, 2008.
- [12] D. Anguelov, D. Koller, E. Parker, and S. Thrun, "Detecting and modeling doors with mobile robots," in *Robotics and Automation, 2004. Proceedings. ICRA'04. 2004 IEEE International Conference on*, vol. 4. IEEE, 2004, pp. 3777–3784.
- [13] S. Hutchinson and T. Bretl, "Robust optimal deployment of mobile sensor networks," in *Robotics and Automation (ICRA), 2012 IEEE International Conference on*, 2012, p. 671676.
- [14] M. Schwager, D. Rus, and J.-J. Slotine, "Decentralized, adaptive coverage control for networked robots," *The International Journal of Robotics Research*, vol. 28, no. 3, pp. 357–375, 2009.
- [15] H. Park and S. Hutchinson, "Robust optimal deployment in mobile sensor networks with peer-to-peer communication," in *Robotics and Automation (ICRA), 2014 IEEE International Conference on*. IEEE, 2014, pp. 2144–2149.

- [16] M. I. Shamos and D. Hoey, "Closest-point problems," in *Foundations of Computer Science, 1975., 16th Annual Symposium on.* IEEE, 1975, pp. 151–162.
- [17] J. Beardwood, J. H. Halton, and J. M. Hammersley, "The shortest path through many points," in *Mathematical Proceedings of the Cambridge Philosophical Society*, vol. 55, no. 04. Cambridge Univ Press, 1959, pp. 299–327.
- [18] S. M. LaValle, *Planning algorithms*. Cambridge university press, 2006.
- [19] M. S. Arulampalam, S. Maskell, N. Gordon, and T. Clapp, "A tutorial on particle filters for online nonlinear/non-gaussian bayesian tracking," *IEEE Transactions on signal processing*, vol. 50, no. 2, pp. 174–188, 2002.
- [20] D. Crisan and A. Doucet, "A survey of convergence results on particle filtering methods for practitioners," *IEEE Transactions on signal processing*, vol. 50, no. 3, pp. 736–746, 2002.
- [21] H. M. Choset, *Principles of robot motion: theory, algorithms, and implementation*. MIT press, 2005.
- [22] P. Berg, L. Norin, and J. Olsson, "Creation of a high resolution precipitation data set by merging gridded gauge data and radar observations for sweden," *Journal of Hydrology*, vol. 541, pp. 6–13, 2016.
- [23] D. Portugal and R. Rocha, "A survey on multi-robot patrolling algorithms," in *Doctoral Conference on Computing, Electrical and Industrial Systems*. Springer, 2011, pp. 139–146.